IRAQI JOURNAL OF APPLIED PHYSICS
Vol. 22, No. 2, April-June 2026, pp. 171-177

Enhanced OLED Efficiency via Gold Nanoparticles-Doped PEDOT:PSS as a Hole Injection Layer

Nawras A. Salman [1,2*]
Estabraq T. Abdullah [3]

[1] Institute of Laser for Postgraduate Studies, University of Baghdad, Baghdad, IRAQ
[2] Department of Medical Physics, College of Applied Sciences, University of Fallujah, Fallujah, IRAQ
[3] Department of Physics, College of Science, University of Baghdad, Baghdad, IRAQ
* Corresponding author email: nouras.ali2101p@ilps.uobaghdad.edu.iq

In this work, organic light-emitting diodes (OLEDs) were fabricated with a modified hole injection layer (HIL) by incorporating gold nanoparticles (AuNPs) into poly(3,4-ethylenedioxythiophene): polystyrene sulfonate (PEDOT:PSS). AuNPs with an average size of ~30 nm was introduced at different volume ratio to investigate their influence on charge injection and electroluminescence performance. The optimized device with a 1:4 AuNPs/PEDOT:PSS ratio achieved a reduced turn-on voltage of 2.2 V and significantly enhanced luminance compared to the pristine device. These improvements are attributed to localized surface plasmon resonance (LSPR), which promotes charge balance, exciton generation, and radiative recombination. Electroluminescence spectra showed broadened emission over 300–800 nm with tunable correlated color temperatures (2000–3500 K). This study demonstrates that embedding AuNPs into PEDOT:PSS offers a simple and scalable strategy for improving OLED efficiency and advancing next-generation optoelectronic devices.

Keyword: Semiconductors; Electroluminescence; OLEDs; Alq3 complex
Received: 17 July 2025; Revised: 24 August 2025; Accepted: 31 August 2025

1. Introduction

Over the past decades, the emergence of organic light-emitting diodes (OLEDs) has revolutionized the field of organic optoelectronics, this advancement has opened new horizons for modern technologies such as digital displays, solid-state lighting, various sensors, and flexible electronic devices [1-4]. Their outstanding electro-optical characteristics, combined with cost-effective fabrication processes, make OLEDs highly attractive for a wide range of industrial applications. Consequently, leading manufacturers have developed display devices. They offer enhanced contrast, wide-angle visibility, energy efficiency, and can be fabricated into ultra-thin, lightweight, and flexible formats. [5-7]. Despite the promising potential of OLED technology, two major challenges persist: enhancing efficiency and lowering fabrication costs. Addressing these issues requires a collaborative initiative between academics and industry to create innovative materials and refine device layouts, thereby improving performance, increasing device lifespans and decreasing power consumption [8-10]. In OLEDs, hole transport layers (HTLs) are essential for minimizing exciton quenching at the anode/emissive layer (EML) interface and for promoting effective hole injection through optimum alignment of interfacial energy [9-12]. An appropriately designed HTL ensures enhanced and balanced hole injection, which increases the radiative electron–hole recombination rate while lowering the operating voltage of the device. Moreover, the HTL functions as an efficient barrier against electron backflow from the EML toward the anode, which contributes to improved device performance [12-17]. However, pristine PEDOT:PSS exhibits limited conductivity and stability, which restricts its ability to provide efficient charge injection. Alternative inorganic HTLs (e.g., MoO_3, NiO, and ZnO) have shown improvements but often require high-temperature deposition or complex fabrication steps, making them less compatible with large-scale processing [18-23].

Recent advances in nanotechnology have provided new opportunities for improving OLEDs by integrating metallic nanoparticles with localized surface plasmon resonance (LSPR). Gold nanoparticles (AuNPs), in particular, are of great interest due to their high stability, tunable plasmonic properties, and compatibility with organic semiconductors. The plasmonic effect of AuNPs can reduce the hole injection barrier, enhance the local electric field, and promote exciton generation and radiative recombination, thereby improving both luminance and efficiency. While some studies have explored plasmonic nanoparticles in OLED architectures, limited research has focused on embedding AuNPs directly into PEDOT:PSS as a hole injection layer. Recent advances in nanotechnology have created new opportunities for enhancing OLED performance

through the incorporation of metallic nanoparticles that exhibit LSPR is a phenomenon that occurs when conduction electrons in metallic nanostructures oscillate collectively in resonance with the electromagnetic field of incoming light. Under incident electromagnetic radiation, resulting in strong optical absorption, field enhancement, and efficient light–matter interaction at the nanoscale. These unique plasmonic properties can be exploited in optoelectronic devices to improve charge injection, carrier balance, and light outcoupling efficiency [24]. Among various plasmonic materials, gold nanoparticles (AuNPs) are particularly attractive due to their excellent chemical stability, biocompatibility, tunable size- and shape-dependent optical properties, and high compatibility with organic semiconductors. Incorporating AuNPs into OLED architectures offers multiple advantages: (i) reducing the hole injection barrier by modifying the interfacial energy alignment, (ii) enhancing the local electric field at the organic/metal interface, which promotes efficient exciton generation, and (iii) increasing the radiative recombination rate, thereby improving luminance and overall device efficiency [25]. Furthermore, AuNPs can act as scattering centers, broaden the emission spectrum and potentially enable white-light generation.

Although several studies have investigated plasmonic nanoparticles such as Ag, Au, and bimetallic nanostructures in OLED configurations, most efforts have focused on incorporating these nanoparticles either into the emissive layer or as external scattering layers to enhance light extraction [27-26]. The aim of this work is to investigate the effect of embedding gold nanoparticles (AuNPs) into PEDOT:PSS as a hole injection layer on the electrical and optical performance of OLEDs. By varying the AuNPs concentration, we seek to optimize charge injection, reduce turn-on voltage, and enhance electroluminescence efficiency.

2. Experimental Part

Organic polymers were supplied from OSSILA, UK Chemical Co. The PEDOT:PSS aqueous solution (CAS No. 155090-83-8) was used as the hole injection material, with water as solvent, sheet resistance of ~10^6 Ω/sq, and a work function of 5.0–5.2 eV. Poly(9,9-di-n-octylfluorenyl-2,7-diyl) (PFO, CAS No. 19456-48-5) was employed as the emissive polymer, soluble in toluene. Tris(8-hydroxyquinoline) aluminum (Alq_3, CAS No. 2085-33-8, molecular weight 459.43 g/mol) was used as the electron transport material, with reported HOMO and LUMO energy levels of 5.62 eV and 2.85 eV, respectively.

The fabrication of OLED devices began with the preparation of the hole transport layer (HTL) by blending gold nanoparticles (AuNPs, ~30 nm in size) with PEDOT:PSS at two volume ratios; 1:2 and 1:4. The mixtures were diluted in distilled water and thoroughly mixed to ensure homogeneity. Pre-cleaned indium tin oxide (ITO)-coated glass substrates were fixed onto a spin-coating apparatus, and the AuNPs-doped PEDOT: PSS solution was deposited at a spin speed of 2000 rpm for 20 seconds. The coated substrates were then thermally annealed at 120 °C for one hour to evaporate residual solvents and form a uniform nanocomposite HTL. Phase segregation during annealing resulted in the migration of AuNPs toward the upper surface of the PEDOT:PSS layer, enhancing its hole injection characteristics. Subsequently, the chemical structures of the organic materials employed in the fabrication of OLED devices - PEDOT:PSS (HTL), PFO (EML), and Alq_3 (ETL) are shown in Fig. (1).

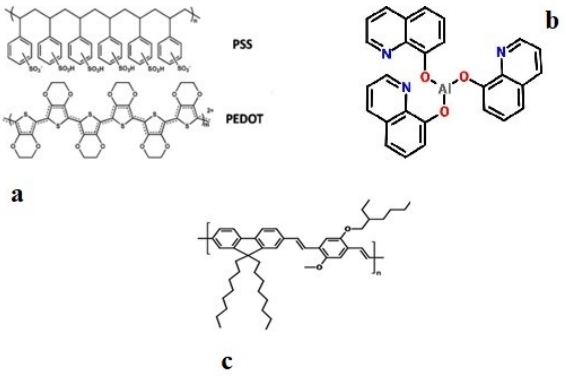

Fig. (1) Chemical structures of (a) PEDOT: PSS (b) Alq_3 (c) PFO

A layer of poly(9,9-di-n-octylfluorenyl-2,7-diyl) (PFO) was deposited on top of the HTL by spin coating at 2000 rpm for 20 seconds. The film was then baked in a convection oven at 60 °C for one hour to ensure solvent removal and film stability. Finally, a layer of tris(8-hydroxyquinoline) aluminum (Alq_3) was deposited using the same spin coating parameters (2000 rpm, 20 seconds), followed by thermal drying at 60 °C for another hour to c complete the formation of the emissive and electron transport layers [28-30]. The fabrication of the device depicted in Fig. (2) was preceded by a series of preparatory procedures. Finally, the multilayer hybrid film (ITO/PEDOT:PSS/PFO/Alq_3/Al).

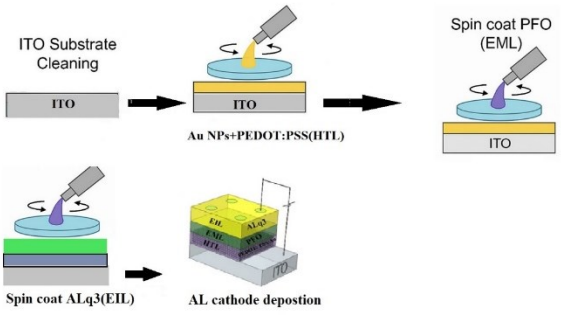

Fig. (2) The experimental setup for OLED fabrication step

OLED devices include of organic layers situated between an anode and a cathode, subjected to opposite biases. Indium tin oxide (ITO) acts as the transparent anode, allowing the generated light to pass through while also functioning as the positive electrode. On the other hand, aluminum (Al) serves as the cathode, facilitating efficient electron injection into the LUMO of the organic semiconductor. In organic semiconductors, charge transport is described in terms of molecular orbitals rather than energy bands as in inorganic semiconductors. The highest occupied molecular orbital (HOMO) is typically regarded as the counterpart of the valence band, where holes (h^+) are generated and transported. The lowest unoccupied molecular orbital (LUMO) corresponds to the conduction band, where electrons (e^-) are injected and transported. When an external bias is applied, holes are injected from the anode into the HOMO level, while electrons are injected from the cathode into the LUMO level. The recombination of these charge carriers within the emissive layer leads to the formation of excitons, which subsequently decay radiatively to produce electroluminescence [31]. In multilayer OLED structures, the injection barriers for electrons and holes differ across the organic layers, leading to selective carrier injection into each layer under forward bias As the applied voltage increases, electrons and holes travel the organic medium, resulting in an accumulation of holes in the HOMO and electrons in the LUMO. Due to Coulombic attraction, these charge carriers recombine to form excitons or exciplexes under the influence of the electric field. This recombination process generates electron–hole pairs that release energy in the form of radiation, producing light emission [32,33], as illustrated in Fig. (3).

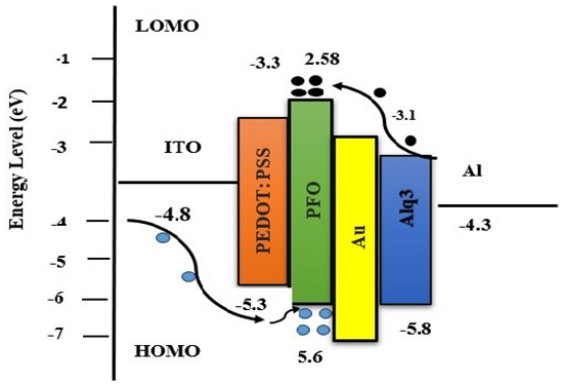

Fig. (3) Work mechanism of ITO/PEDOT:PSS:Au/PFO/Alq3/Al

3. Results and Discussion

The FE-SEM images (Fig. 4a) proved a uniformed dispersion of AuNPs in the matrix of PEDOT:PSS film, with an absence of large aggregates. Cross-sectional FE-SEM (Fig. 4b) showed clearly separated trilayer stack with the thickness of ~915 nm of PEDOT:PSS:Au, 323 nm of PFO and 132 nm of Alq_3 as expected design of the device. The AuNPs inside the PEDOT:PSS layer should serve to build conductive percolation pathways and to enrich the HTL/EML interface by phase segregation, leading to enhanced hole injection efficiency.

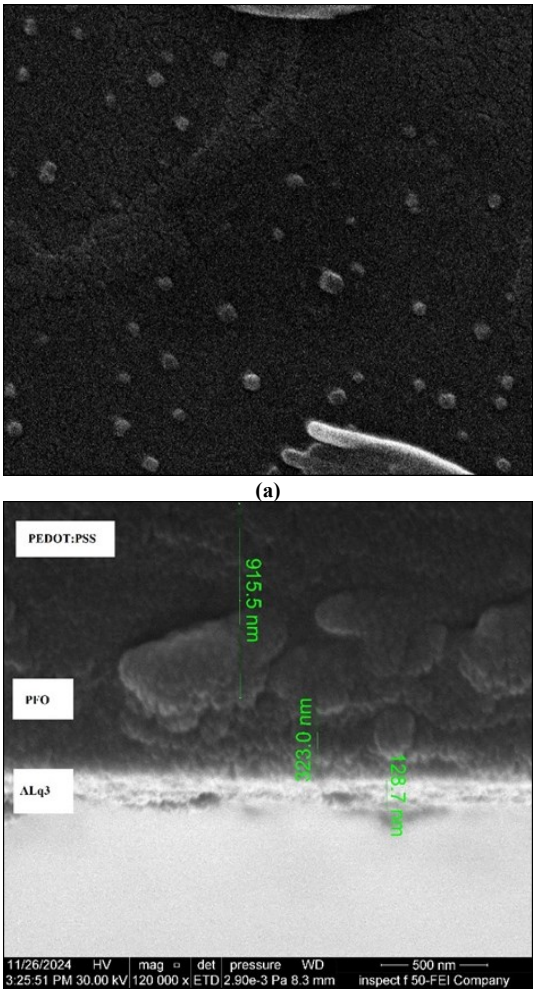

Fig. (4) (a) SEM micrograph of PEDOT:PSS–Au nanocomposite layer on glass substrate, (b) Cross-section view of FE-SEM images of OLED thin films (ITO/PEDOT: PSS/PFO/Alq_3)

Absorption spectra were measured in the 300–800 nm range. As shown in Fig. 5(a-c), a broad band was detected in the near-UV region, which progressively decreased in intensity with increasing wavelength. Distinct absorption peaks were observed at 395 nm for PFO, 388 nm for Alq_3, and 520 nm for AuNPs. These wavelengths were subsequently employed as excitation sources to investigate the photoluminescence (PL) response of PFO, Alq_3, and AuNPs. As presented in Fig. (6a-c), the optical energy gap (E_g) was estimated using the relation E_g (eV) = 1240/λ (nm). For PFO, the first absorption peak observed at 440 nm corresponds to the LUMO–HOMO transition, yielding an energy gap of approximately 2.8 eV [34-36]. Similarly, in the case of Alq_3, the initial peak located at 595 nm represents the LUMO–HOMO transition, with an

estimated gap of about 2.5 eV. For AuNPs, the band-to-band transition at 520 nm provided an energy gap of nearly 3.1 eV.

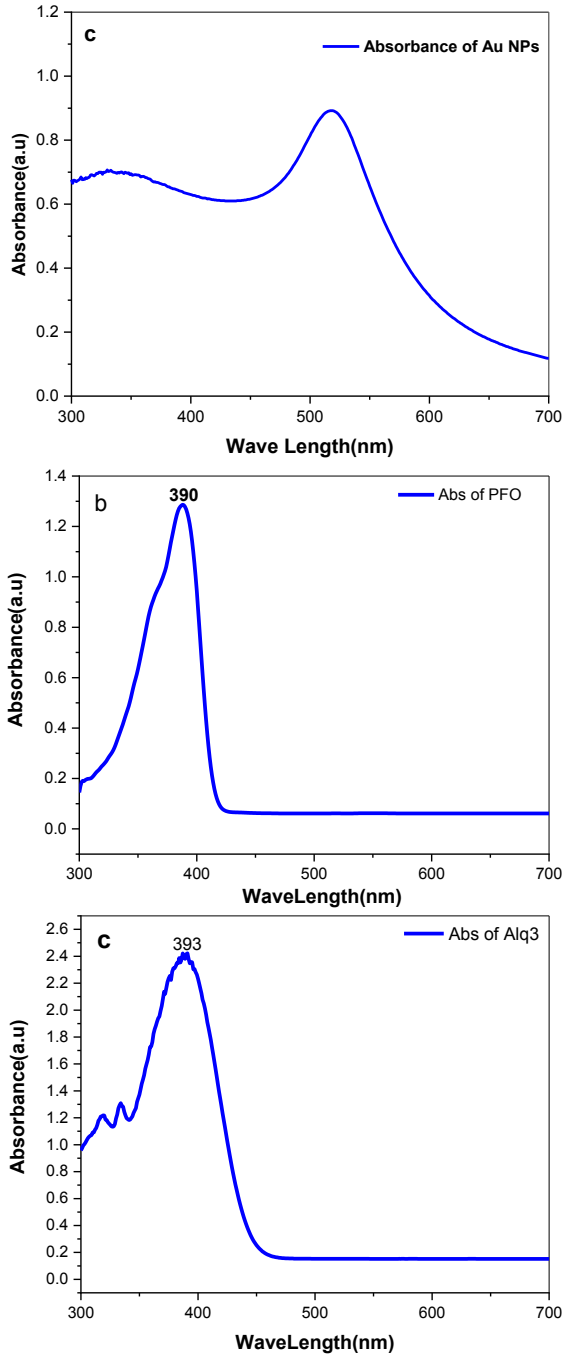

Fig. (5) Absorption spectra of (a) Au NPs, (b) PFO, and (c) Alq_3

The I-V measurements (Fig. 7) showed a remarkable enhancement of hole injection when doped with AuNPs. The pristine OLED showed a V_{on} of 4.5 V; whereas, introduction of AuNPs decreased V_{on} to 3.92 V (1:1 ratio of AuNPs) and 2.28 V (1:4 ratio of AuNPs), reductions of 13% and ~49%, respectively. These enhancements are explained by the decrease in the hole injection barrier and the HTL conductivity increment through the AuNPs nanoscale percolation networks. In addition, the work function matching between AuNPs and PEDOT:PSS also favors charge injection. The OLEDs modified with PEDOT:PSS+AuNPs achieved the highest performance at AuNPs concentration ratios of 1:4 and 1:2.

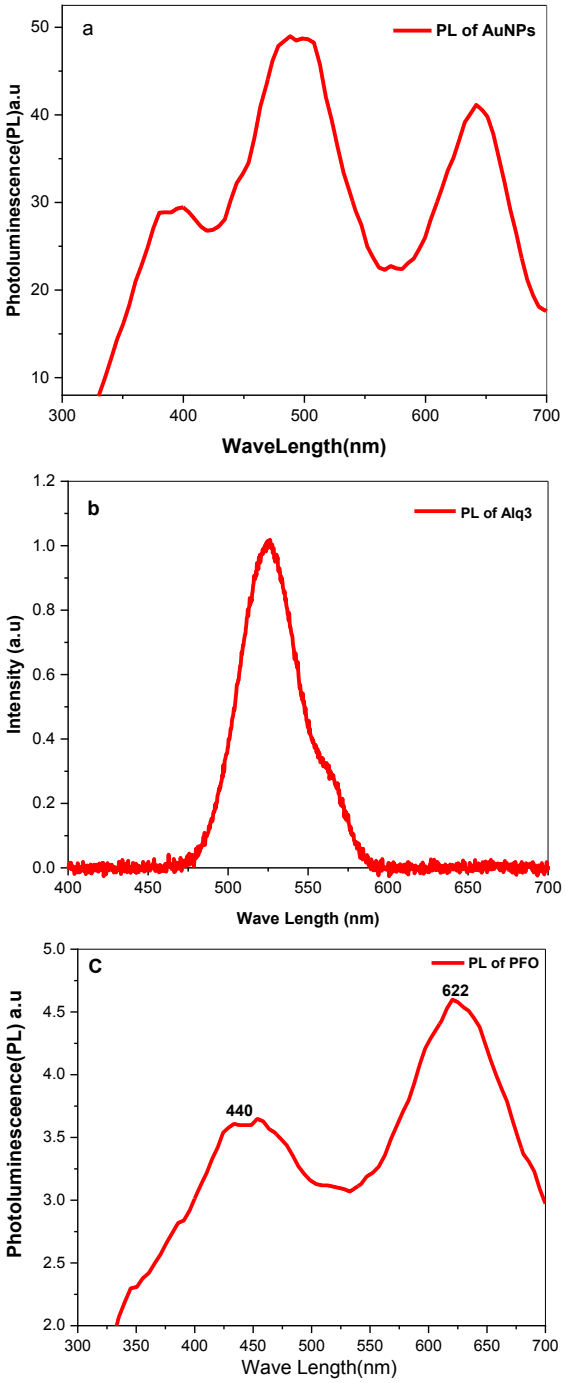

Fig. (6) Photoluminescence spectra of (a) Au NPs, (b) Alq_3, and (c) PFO

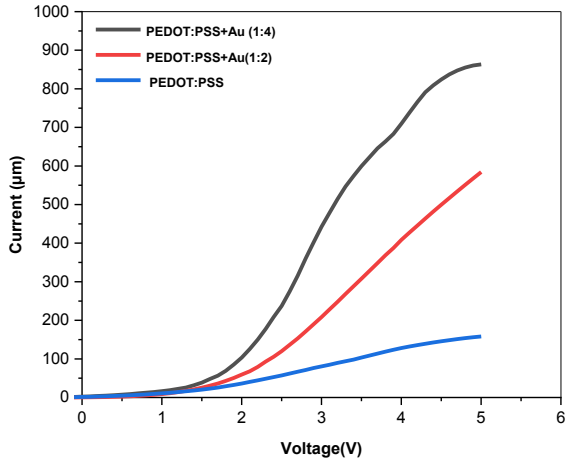

Fig. (7) Current-Voltage characteristics of the fabricated OLEDs based on as-deposited PEDOT:PSS and PEDOT:PSS+Au-NPs at different volume ratios

The OLED fabricated with a PEDOT:PSS:AuNPs ratio of 1:4 exhibited a reduced turn-on voltage of 2.28 V relative to the reference device, whereas the 1:1 ratio device showed an increased value of 3.92 V. In comparison, the reference device achieved a turn-on voltage of 4.5 V, surpassing the other reference device. The improved OLED performance in this work is likely due to the increased current injected into the device by incorporating gold nanoparticles into the injection layer. This enhancement is attributed to the formation of conductive percolation networks formed by the densely distributed AuNPs. Due to their high work function and favorable alignment with the HOMO level of PEDOT:PSS, AuNPs effectively lower the energy barrier for hole injection. Furthermore, they act as nanoscale conductive bridges that promote more efficient charge transport across the hole transport layer. As a result, the current density is markedly increased, reflecting a substantial improvement in overall device conductivity and performance.

The electroluminescence at a bias voltage and the light emission spectrum for the hybrid device were recorded using a photomultiplier detector at room temperature. The light was obtained approximately through ITO/PEDOT:PSS/PFO/Alq_3/Al. The emission spectrum resulted from the effect of adding hybrid PEDOT/PSS-Au solutions as a hole injection layer. As a result, the emission spectrum exhibited enhanced intensity and broader expansion, attributed to the formation of sublevels that caused spectral shifts into the yellow, orange, and red regions. These spectra were recorded under the application of forward-bias voltages. [37-39]. The blue emission at 440 nm corresponds to the emission of PFO, as the band gap of PFO is 2.8 eV. The electroluminescence (EL) spectra of the fabricated OLEDs revealed a clear enhancement in emission intensity and spectral behavior upon doping the PEDOT:PSS layer with gold nanoparticles (AuNPs). The pristine device exhibited a broad emission peak centered around 450 nm, characteristic of the PFO and Alq_3 layers. Doping with AuNPs at 1:2 and 1:4 volume ratios led to a significant increase in EL intensity, with the 1:4 ratio showing the highest brightness. This enhancement is attributed to the localized surface plasmon resonance (LSPR) of AuNPs, which improves hole injection and amplifies the internal electric field, promoting exciton generation and radiative recombination. Additionally, a slight red-shift in the EL peak was observed with increasing AuNPs concentration, indicating a shift in the exciton recombination zone and possible plasmon–exciton coupling. The overall emission spectra extended from 300 to 800 nm are appearing in Fig. (8), and the spectral shape and intensity variations confirm that the AuNPs not only boost luminance but also enable spectral tuning, with correlated color temperature (CCT) values ranging from 2000 to 3500 K depending on the doping level.

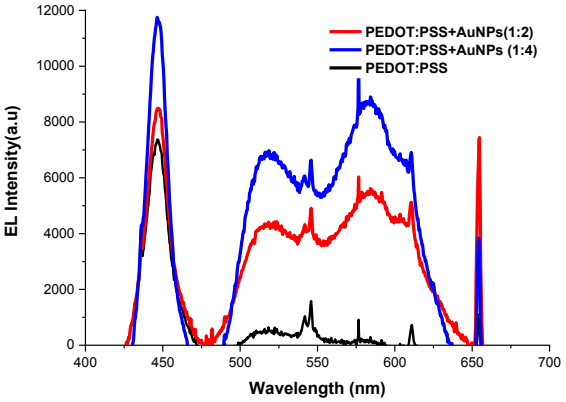

Fig. (8) Normalized electroluminescence (EL) spectra of the same OLEDs at a voltage of 5 V

The electroluminescence (EL) spectra of the devices were evaluated, and the corresponding emission colors were determined using the Commission International de l'Éclairage (CIE) 1931 chromaticity coordinates. Figure (9) shows the electroluminescence spectra that were analyzed according to the CIE1931. The CCT was computed by McCamy's algorithm of approximation and CCT was calculated from using the following equations [40]:

$$CCT = -449n^3 + 3525n^2 - 6823.3n + 5520.33 \quad (1)$$

$$n = \frac{x-0.332}{y-0.1858} \quad (2)$$

Table (1) CCT and xy coordinates for different samples

Sample	x,y	n	CCT (K^0)
ITO/PEDOT:PSS:Au/PFO/Alq_3/Al	0.319, 0.325	-0.0935	12055
ITO/PEDOT:PSS:Au1:2/PFO/Alq_3/Al	0.212, 0.419	-0.502	9882
ITO/PEDOT:PSS:Au1:4/PFO/Alq_3/Al	0.301, 0.436	-0.124	6421

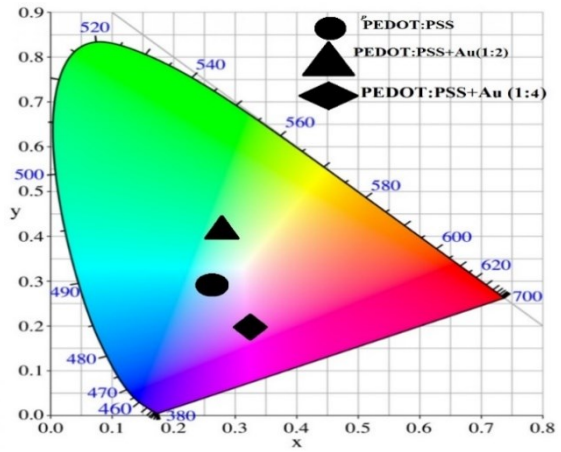

Fig. (8) Coordinates of a multilayer device in the CIE 1931 chromaticity diagram

4. Conclusions

In conclusion, this study shows that adding plasmonic AuNPs to PEDOT:PSS could make it a better HTL for OLEDs with improved performance. Incorporating gold nanoparticles (AuNPs) into PEDOT:PSS significantly enhances OLED performance. Devices with a 1:4 AuNPs ratio exhibited the lowest turn-on voltage (2.28 V) and highest luminance. The plasmonic effects of AuNPs improved charge injection and mitigated efficiency roll-off. Additionally, variations in AuNPs concentration influenced the electroluminescence spectrum and correlated color temperature (CCT). These results confirm that optimizing AuNPs content in the HTL is a practical strategy for enhancing both electrical and optical performance of OLEDs.

References

[1] Y. Karzazi, "Organic light emitting diodes: Devices and applications", *J. Mater. Environ. Sci.*, 5(2) (2014) 1-12.

[2] B. Geffroy, P.L. Roy and C. Prat, "Organic light-emitting diode (OLED) technology: materials, devices and display technologies", *Polymer Int.*, 55(6) (2006) 572-582.

[3] Z. Wu and D. Ma, "Recent advances in white organic light-emitting diodes", *Mater. Sci. Eng. R.*, 107 (2016) 1-42.

[4] G. Schwartz et al., "Harvesting triplet excitons from fluorescent blue emitters in white organic light-emitting diodes", *Adv. Mater.*, 19(21) (2007) 3672-3676.

[5] D. Yokoyama, "Molecular orientation in small-molecule organic light-emitting diodes", *J. Mater. Chem.*, 48 (2011) 19187-19202.

[6] T.-H. Han et al., "Extremely efficient flexible organic light-emitting diodes with modified graphene anode", *Nat. Photonics*, 6(2) (2012) 105-110.

[7] J. Lee et al., "Deep blue phosphorescent organic light-emitting diodes with very high brightness and efficiency", *Nat. Mater.*, 15(1) (2015) 92-98.

[8] X. Li et al., "Room-temperature solution-processed molybdenum oxide as hole transport layer with Ag nanoparticles for highly efficient inverted organic solar cells", *J. Mater. Chem. A*, 22 (2013) 6614-6621.

[9] C.H. Cheung et al., "Determination of carrier mobility in phenylamine by time-of-flight, dark-injection, and thin film transistor techniques", *J. Appl. Phys.*, 103(9) (2008) 093705.

[10] P. Pattanasattayavong et al., "Electronic properties of copper(I) thiocyanate (CuSCN)", *Adv. Electron. Mater.*, 3(3) (2017) 1600378.

[11] M.P. De Jong et al., "Stability of the interface between indium-tin-oxide and PEDOT:PSS in polymer light-emitting diodes", *Appl. Phys. Lett.*, 77(14) (2000) 2255-2257.

[12] M. Jørgensen et al., "Stability/degradation of polymer solar cells", *Sol. Energy Mater. Sol. Cells*, 92(7) (2008) 686–714.

[13] I.M. Ibrahim et al., "Characterization of Au/PS/p-Si heterojunction", *J. Optoelectron. Adv. Mater.*, 16(3-4) (2014) 476-480.

[14] H.A. Abbas, W.C. Koubaa and E.T. Abdullah, "Synthesis, characterization and functionalization of P3HT-CNT nanocomposite thin films with doped Ag_2O", *East Eur. J. Phys.*, 2024(1) (2024) 342-354.

[15] J.H. Kim et al., "High-performance and environmentally stable planar heterojunction perovskite solar cells based on a solution-processed copper-doped nickel oxide hole-transporting layer", *Adv. Mater.*, 27(4) (2014) 695-701.

[16] T. Matsushima, Y. Kinoshita and H. Murata, "Formation of Ohmic hole injection by inserting an ultrathin layer of molybdenum trioxide", *Appl. Phys. Lett.*, 91(25) (2007) 253504.

[17] H. Choi et al., "Conjugated polyelectrolyte hole transport layer for inverted-type perovskite solar cells", *Nat. Commun.*, 6(1) (2015) 7348.

[18] A. Ayobi et al., "The effects of molybdenum trioxide (MoO_3) thickness on the improvement of driving and operating voltages of organic light emitting devices", *Optoelectron. Adv. Mater. Rapid Commun.*, 13 (2019) 519-524.

[19] J. Liu et al., "Efficient inverted top-emitting organic light-emitting devices with double electron injection layers", *Opt. Laser Technol.*, 117 (2019) 260-264.

[20] Y. Guo et al., "Improved efficiency of organic light emitting devices using graphene oxide with optimized thickness as hole injection layer", *Solid-State Electron.*, 153 (2018) 46-51.

[21] Y. Zhang et al., "Aqueous solution-processed vanadium oxide for efficient hole injection interfacial layer in organic light-emitting diode", *phys. stat. sol. a*, 215(11) (2018) 1800047.

[22] W. Li et al., "Solution-processed WOx hole injection layer for efficient fluorescent blue organic light-emitting diode", *Curr. Appl. Phys.*, 18(5) (2018) 583-589.
[23] J. Kim et al., "Solution-processed nickel oxide nanoparticles with NiOOH for hole injection layers of high-efficiency organic light-emitting diodes", *Nanoscale*, 8(40) (2016) 17608-17615.
[24] Z. Liang et al., "Plasmonic enhanced optoelectronic devices", *Plasmonics*, 9(4) (2014) 859-866.
[25] H. Lian et al., "Recent advances in the optimization of organic light-emitting diodes with metal-containing nanomaterials", *Chem. Rec.*, 19(1) (2019) 1-16.
[26] H. Choi et al., "Versatile surface plasmon resonance of carbon-dot-supported silver nanoparticles in polymer optoelectronic devices", *Nat. Photonics*, 7(9) (2013) 732-738.
[27] X. Gu et al., "Light-emitting diodes enhanced by localized surface plasmon resonance", *Nanoscale Res. Lett.*, 6 (2011) 199.
[28] A.N. Naje, O.A. Ibrahim and E.T. Abdullah, "Blue organic-inorganic light emitting diode based on electroluminescence CdS nanoparticle", *Iraqi J. Sci.*, 64(12) (2023) 6277-6284.
[29] H.R. Mohammed and A.N. Naje, "Preparation of hybrid light-emitting diodes (OI-LED) based on carbon nanoparticles", *Iraqi J. Phys.*, 23(2) (2025) 128-137.
[30] N.A. Salman and E.T. Abdullah, "Synthesis and hybridization of gold@silver core/shell nanoparticles via pulsed laser ablation", *Semiconductors*, 59(6) (2025) 513-520.
[31] A. Islam et al., "A review on fabrication process of organic light emitting diodes", Bangladesh University of Engineering and Technology (2013).
[32] H. Yersin, "Triplet emitters for OLED applications. Mechanisms of exciton trapping and control of emission properties", *Top. Curr. Chem.*, 241 (2012) 1-26.
[33] S. Chen et al., "Efficient, color-stable flexible white top-emitting organic light-emitting diodes", *Org. Electron.*, 14(11) (2013) 3037-3045.
[34] S.F. Haddawi et al., "Vertically emitted dual wavelength random laser based on light emitting polymers and silver nanowires double cavity structure", *Optik*, 219 (2020) 165256.
[35] F. Guo et al., "The fabrication of color-tunable organic light-emitting diode displays via solution processing", *Light Sci. Appl.*, 6 (2017) e17094.
[36] G. Lozano et al., "Metallic nanostructures for efficient LED lighting", *Light Sci. Appl.*, 5 (2016) e16080.
[37] N. Gupta et al., "Efficiency enhancement in blue organic light emitting diodes with a composite hole transport layer based on PEDOT:PSS doped with TiO_2 nanoparticles", *Displays*, 39 (2015) 104-108.
[38] A.C. Bhowal, H. Talukdar and S. Kundu, "Preparation, characterization and electrical behaviors of PEDOT:PSS-Au/Ag nanocomposite thin films", *Polym. Bull.*, 76 (2019) 5233-5251.
[39] K. Khurana and N. Jaggi, "Localized surface plasmonic properties of Au and Ag nanoparticles for sensors: A review", *Plasmonics*, 16 (2021) 981–999.
[40] C.S. McCamy, "Correlated color temperature as an explicit function of chromaticity coordinates", *Color Res. Appl.*, 17(2) (1992) 142-144.

